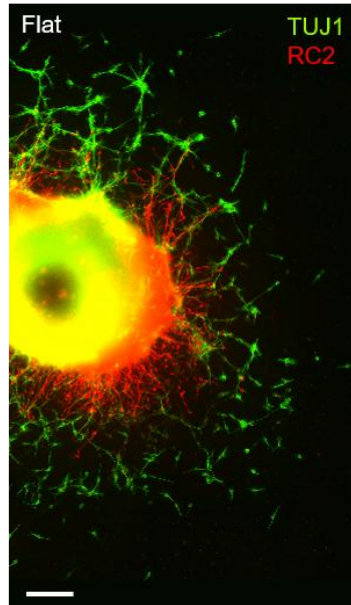
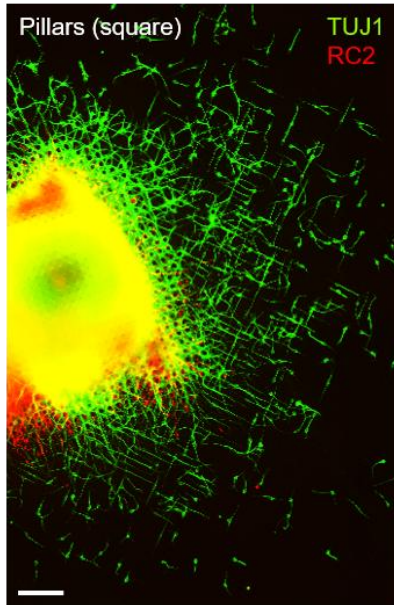
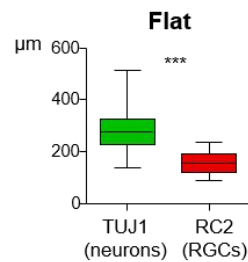
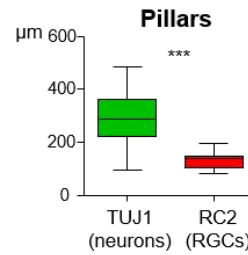


Biomaterials SUPPORTING INFORMATION

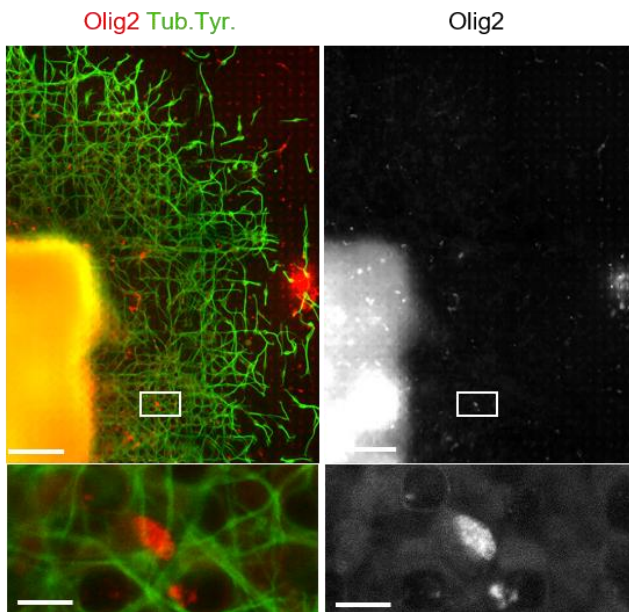
A Radial glial cells



B Distance to the explant

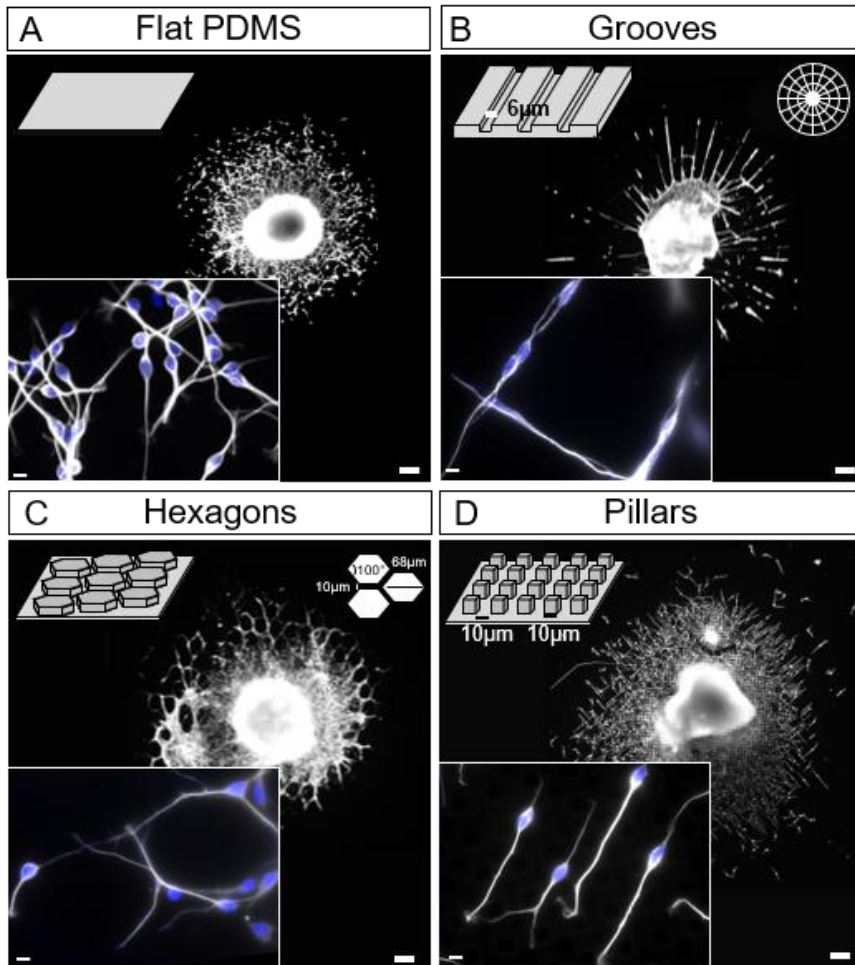


C Oligodendrocytes progenitors

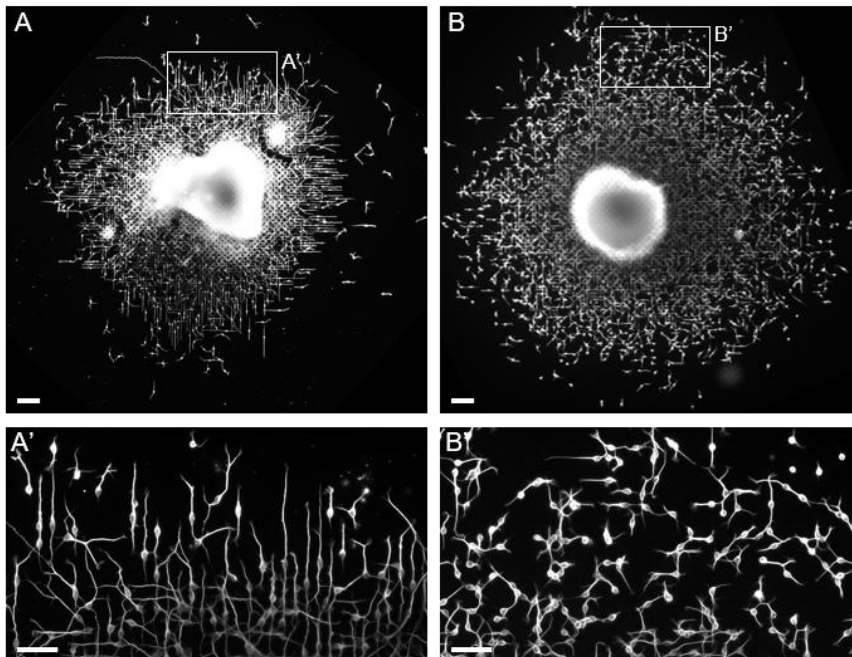


Supplementary figure 1: Cellular composition of the cultures

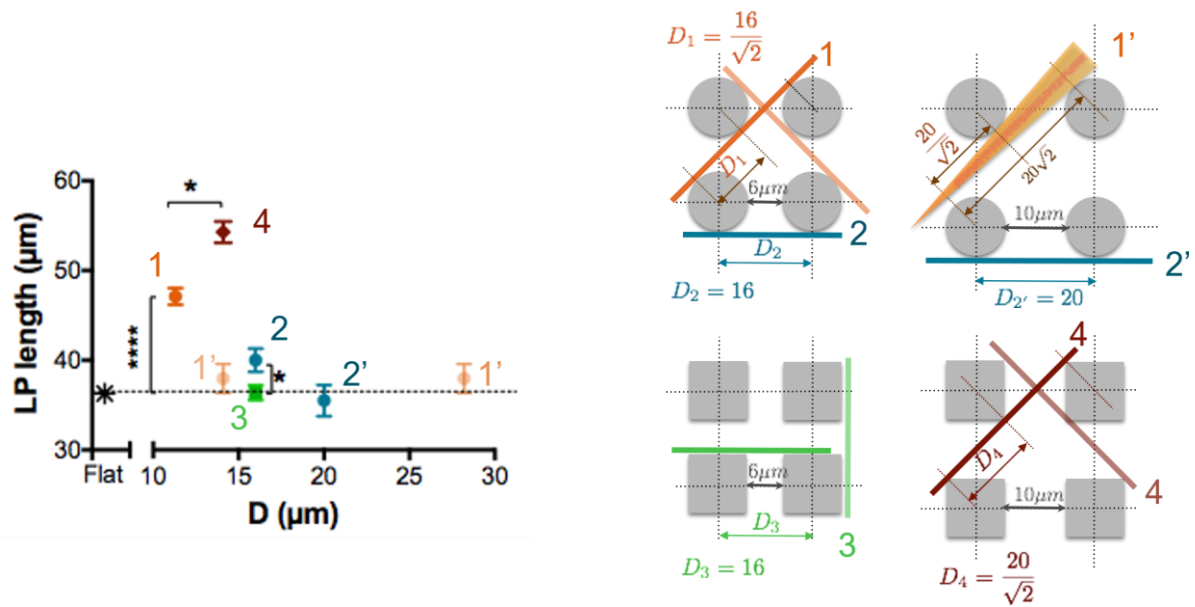
(A) Immunostaining against betaIII tubulin (post-mitotic neurons, green) and RC2 (radial glial cells, red) after 24 hours of culture on square pillars (left) or flat PDM (right). Scale 100 μ m (B) Measure of distances from the explant reached by betaIII tubulin + cells or RC2+ cells on pillars (no differences were observed between square and round pillars and they were thus grouped) or flat PDMS. In both conditions, RC2+ fibers stay confined close to the explant. Pillars: betaIII tubulin n=53 explants, 2 cultures. RC2 n=12 explants, 1 culture. Flat: betaIII tubulin n=35 explants, 2 cultures. RC2 n=9 explants, 2 cultures. T-test. (C) Immunostaining against Olig2 (oligodendrocytes progenitors, red) and tyrosinated tubulin (green) on square pillars showing that Olig2+ progenitors stay confined within or close to the explant. The same result was obtained on round pillars or flat PDMS. Scale 100 μ m, 10 μ m (enlarged views) Scale 100 μ m



Supplementary figure 2: Migration of interneurons on microstructures with different geometries
 Explants (white spot in the center of cultures) surrounded by migratory interneurons were fixed after 24 hours in culture. Explants were cultured on either (A) flat PDMS, (B) grooves (width 6 μm , height 10 μm), (C) hexagons (length 68 μm separated by 10 μm), or (D) square pillars (10 μm size and height separated by 10 μm). Interneurons are visualized by tyrosinated tubulin immunostaining (white). Inserts show enlarged views of interneurons at the periphery of the migration area (Dapi staining of the nucleus, blue). Scale bars, 100 μm (low magnification picture), 10 μm (inserts).

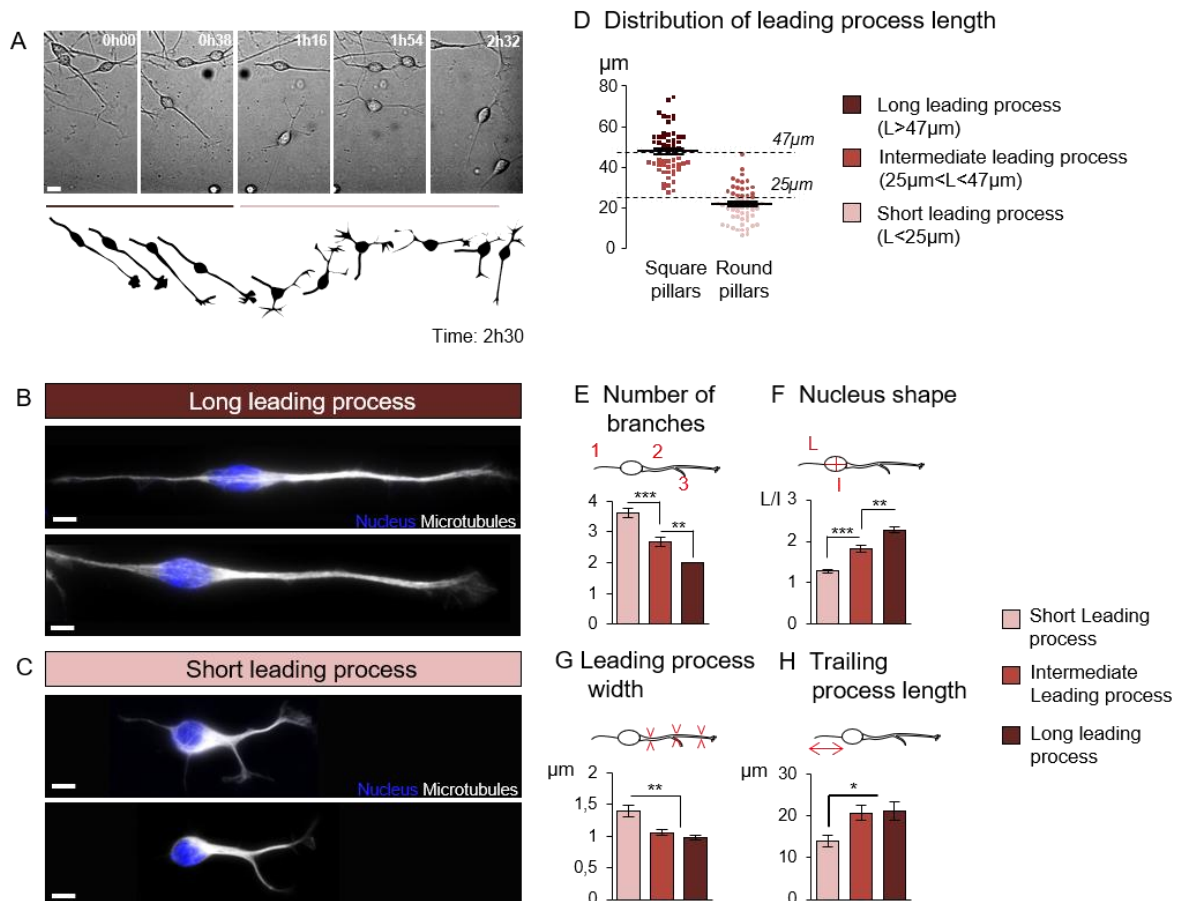


Supplementary figure 3: Classification of cultured explants according to the macroscopic organization of migratory interneurons
 (A,B) Explants fixed after 24h in culture show two main types of macroscopic organization of interneurons at the periphery of their migration area (A',B'), either long and aligned (A,A') or short and non-aligned (B,B'). Scale bars, 100 μm (A,B), 50 μm (A', B')



Supplementary figure 4: Leading process length of unipolar cells in different orientations in between the different configurations of pillars

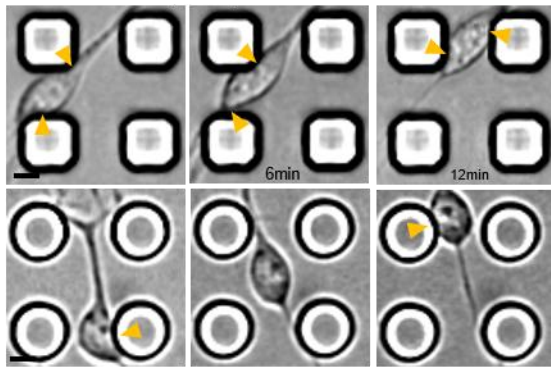
The length of leading processes of unbranched cells were extracted for interneurons in different orientations (orthogonal or diagonal). The different LP length are represented as a function of D which represents the distance between the potential contact points the LP can establish with the topographies according to the main orientations selected by the shape and distribution of pillars (see the schemes on the right, see also the graphs of Figure 2). 10 µm spaced round pillars represent a particular case as the angular width of the peaks associated to the LP diagonal orientation defines two possible distances D1', which we choose to represent in light orange on both graph and scheme. Flat: 280 cells, D1: 147 cells, D2: 96 cells, D3: 240 cells, D4: 243 cells, D1': 70 cells, D2': 47 cells. Significance of differences was assessed using a non-parametric ANOVA, Dunn's post test.



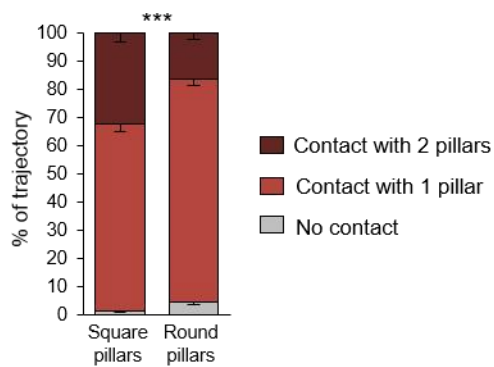
Supplementary figure 5: Characterization of two morphological states of migrating interneurons

(A) Frames from the time lapse sequence of an interneuron migrating on a flat surface (top) and drawing of the same sequence (bottom, total duration 2h30). The interneuron exhibited successively two opposite morphological organizations, long unipolar and then, short multipolar. Scale bar, 10µm. (B,C) High magnification views of tyrosinated tubulin (white) and Dapi (blue) labeled interneurons exhibiting those two morphologies. Scale bars, 5µm. (D) Distribution of leading process lengths in interneurons migrating on either square or round pillars (55 long and unbranched cells from 6 cultures on square pillars and 56 short and branched cells from 4 cultures on round pillars) shows that interneurons with the longest non-branched leading process were observed on the square pillars, and multipolar interneurons with the shortest processes, on the round pillars. Intermediate lengths were observed on both substrates. (E-H) Interneurons migrating on pillared surfaces were distributed in 3 classes according to the length of their leading process, whatever their morphology (branched, non-branched) and the shape of the pillars (28 cells with a long leading process (6 cultures), 46 cells with intermediate lengths (10 cultures), 37 cells with short leading processes (5 cultures)). In each class, the mean number of branches (E), the nucleus shape (F) defined by the ratio of the long and short axes, the mean width of the leading process (G) (average of 3 measures along the whole length of the LP) and the mean trailing process length (H) were measured. Significance of differences was assessed using a non-parametric ANOVA, Dunn's post test (***) $p < 0.0001$ in E, F, (**) $p = 0.0004$ in G, (*) $p = 0.0069$ in H). Error bars represent mean \pm SEM.

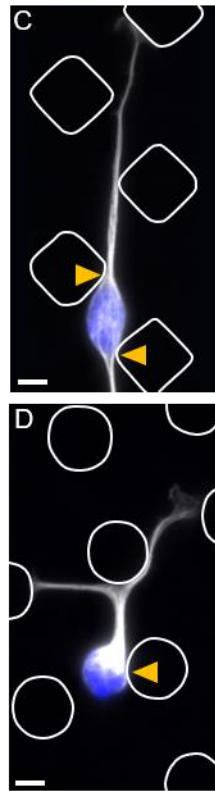
A Sequences of nucleus movement



B Time of contact with the pillars

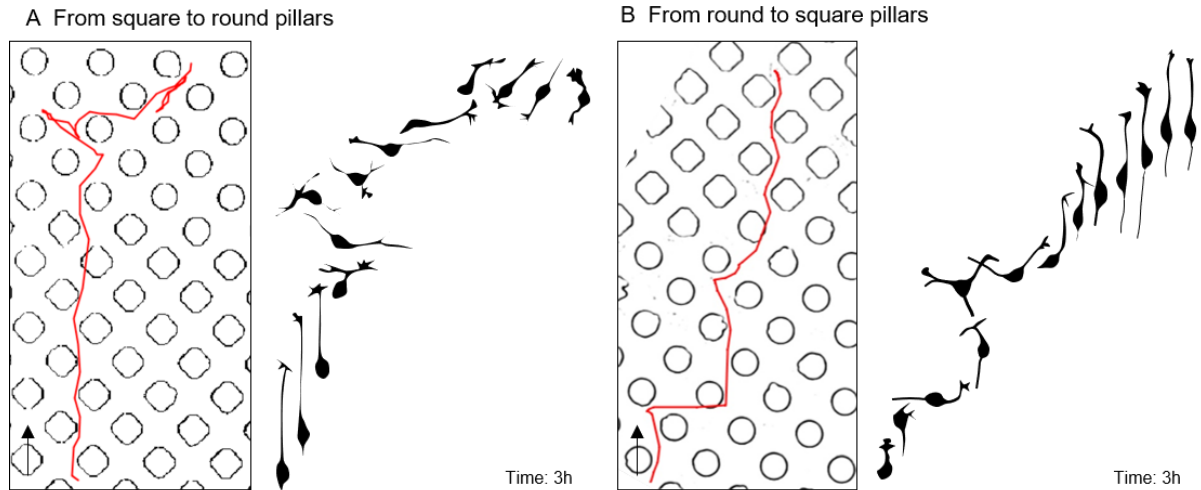


Dapi Tub.Tyr



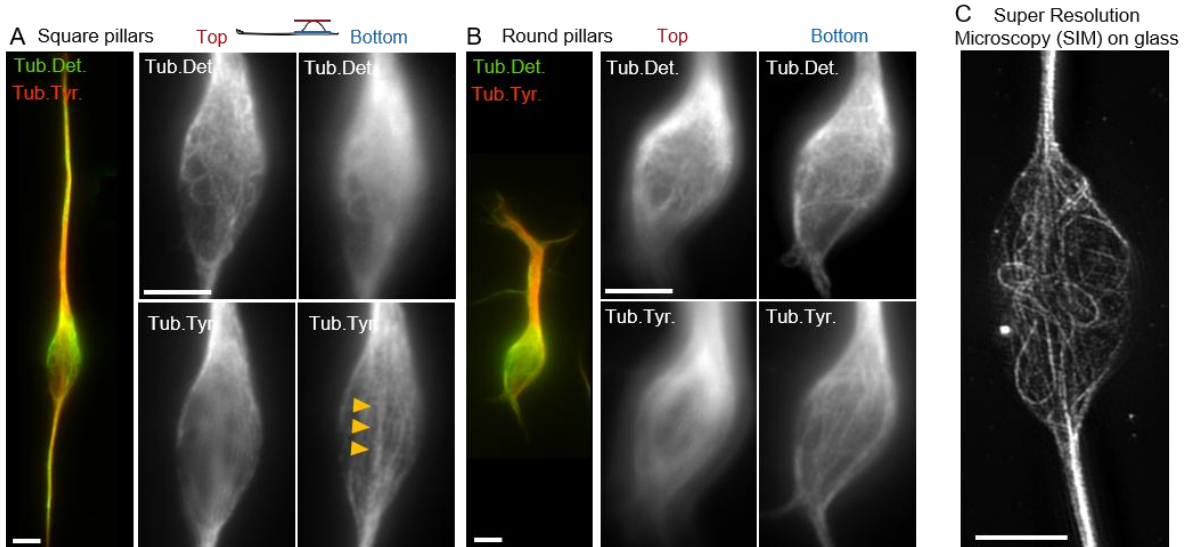
Supplementary figure 6: Cell body interaction with the microstructures

(A) Time lapse sequences recorded with a phase contrast microscope showing somal movements in migrating interneurons (top, on square pillars, bottom, on round pillars). Yellow arrows indicate contacts between the cell body and the pillars. Scale bars, 10 μ m. (B) The time of contact of the cell body with no, one or two pillars is noted on each frame and expressed as a percentage of the total trajectory duration. Contact durations significantly differed on square pillars (30 cells from 6 cultures) and round pillars (30 cells from 5 cultures) (Chi2 test, ***, $p < 0.0001$). Error bars represent mean \pm SEM. (C,D) Immunostaining of tyrosinated tubulin (white) and Dapi staining (blue) in representative interneurons that migrated on square (C) and round (D) pillars. Pillars were drawn from phase contrast pictures. Contacts between the cell body and the pillars are indicated by arrow heads (yellow). Scale bars, 5 μ m.



Supplementary figure 7: Interneuron trajectories and morphologies from square to round/round to square pillars

(A) Trajectory of an interneuron migrating from square to round pillars (left) and drawing of the corresponding cell shape (right). Total time: 3h. Interval between frames: 15 minutes. (B) Trajectory of an interneuron migrating from round to square pillars (left) and drawing of the corresponding cell shape (right). Total time: 3h. Interval between frames: 15 minutes. Examples of such changes in behavior were observed on 4 independent experiments



Supplementary figure 8: Microtubules network architecture in the cell body

(A,B) Interneurons were immunostained with antibodies against tyrosinated tubulin (dynamic microtubules, red) and detyrosinated tubulin (stable microtubules, green). Panels show maximum projections of epifluorescence microscopy pictures acquired at the top (left) or at the bottom (against the substrate, right) of the cell body. (C) Super resolution microscopy (SIM) shows the organization of stable microtubules (detyrosinated tubulin) in the cell body of an interneuron that migrated on a flat glass coverslip. Scale bars, 5 μ m.

Captions of Movies

Movie 1 related to Figure 4: phase contrast recording with a X20 objective (NA, 0.7) of symmetric growth cone splitting in between round pillars. Interval between frames: 115 seconds. Yellow arrows indicate the formation of two equivalent sister branches

Movie 2 related to Figure 4: phase contrast recording with a X20 objective (NA, 0.7) of asymmetric growth cone splitting in between square pillars. Interval between frames: 105 seconds. Yellow arrow indicates the formation of a thin lateral branch

Movies 3, 4, 5 related to Figure 5: phase contrast recording with a X20 objective (NA, 0.7) of interneuron migration in between square pillars (Movie 4), flat surface (Movie 3) or round pillars (Movie 5). Interval between frames: 115 seconds

Movie 6 related to Figure 6: phase contrast recording with a X20 objective (NA, 0.7) of the growth cone movement in between square pillars. Interval between frames: 115 seconds. Red dots show the leading process tip (LPT) tracked for the analysis.

Movie 7 related to Figure 6: phase contrast recording with a X20 objective (NA, 0.7) of the growth cone movement in between round pillars. Interval between frames: 115 seconds. Red dots show the leading process tip (LPT) tracked for the analysis

Movie 8 related to Figure S4A: phase contrast recording with a X20 objective (NA, 0.7) of cell body navigation in between square pillars. Interval between frames: 90 seconds. Yellow arrows indicate the contacts between the cell body and the pillars

Movie 9 related to Figure S4A: phase contrast recording with a X20 objective (NA, 0.7) of cell body navigation in between round pillars. Interval between frames: 105 seconds. Yellow arrows indicate the contacts between the cell body and the pillars

Movies 10 et 11 related to figure S7: phase contrast recording with a X20 objective (NA, 0.7) of interneuron migration from square to round (Movie10) or round to square (Movie11) pillars. Interval between frames: 3 minutes (Movie10), 5 minutes (Movie11).